

Hepatitis C Virus Mediated Changes in miRNA-449a Modulates Inflammatory Biomarker YKL40 through Components of the NOTCH Signaling Pathway

Nayan J. Sarma¹, Venkataswarup Tiriveedhi¹, Vijay Subramanian¹, Surendra Shenoy¹, Jeffrey S. Crippin³, William C. Chapman¹, Thalachallour Mohanakumar^{1,2*}

1 Department of Surgery, Washington University School of Medicine, Saint Louis, Missouri, United States of America, **2** Department of Pathology & Immunology, Washington University School of Medicine, Saint Louis, Missouri, United States of America, **3** Department of Medicine, Washington University School of Medicine, Saint Louis, Missouri, United States of America

Abstract

Liver disease due to hepatitis C virus (HCV) infection is an important health problem worldwide. HCV induced changes in microRNAs (miRNA) are shown to mediate inflammation leading to liver fibrosis. Gene expression analyses identified dysregulation of miRNA-449a in HCV patients but not in alcoholic and non-alcoholic liver diseases. By sequence analysis of the promoter for *YKL40*, an inflammatory marker upregulated in patients with chronic liver diseases with fibrosis, adjacent binding sites for nuclear factor of Kappa B/P65 and CCAAT/enhancer-binding protein alpha (CEBP α) were identified. P65 interacted with CEBP α to co-operatively activate *YKL40* expression through sequence specific DNA binding. *In vitro* analysis demonstrated that tumor necrosis factor alpha (TNF α) mediated *YKL40* expression is regulated by miRNA-449a and its target *NOTCH1* in human hepatocytes. *NOTCH1* facilitated nuclear localization of P65 in response to TNF α . Further, HCV patients demonstrated upregulation of *NOTCH1* along with downregulation of miRNA-449a. Taken together it is demonstrated that miRNA-449a plays an important role in modulating expression of *YKL40* through targeting the components of the NOTCH signaling pathway following HCV infection. Therefore, defining transcriptional regulatory mechanisms which control inflammatory responses and fibrosis will be important towards developing strategies to prevent hepatic fibrosis especially following HCV recurrence in liver transplant recipients.

Citation: Sarma NJ, Tiriveedhi V, Subramanian V, Shenoy S, Crippin JS, et al. (2012) Hepatitis C Virus Mediated Changes in miRNA-449a Modulates Inflammatory Biomarker YKL40 through Components of the NOTCH Signaling Pathway. PLoS ONE 7(11): e50826. doi:10.1371/journal.pone.0050826

Editor: Partha Mukhopadhyay, National Institutes of Health, United States of America

Received: September 4, 2012; **Accepted:** October 25, 2012; **Published:** November 30, 2012

Copyright: © 2012 Sarma et al. This is an open-access article distributed under the terms of the Creative Commons Attribution License, which permits unrestricted use, distribution, and reproduction in any medium, provided the original author and source are credited.

Funding: This work was supported by the Barnes-Jewish Foundation at Barnes-Jewish Hospital, St. Louis, MO. The funders had no role in study design, data collection and analysis, decision to publish, or preparation of the manuscript.

Competing Interests: The authors have declared that no competing interests exist.

* E-mail: kumart@wustl.edu

Introduction

Liver diseases resulting from hepatitis C virus (HCV) infection is a major health issue worldwide as well as the United States [1,2]. It is estimated that about 4 million people are infected with HCV in the United States and about 300 million worldwide [1]. The natural history of HCV infection in the liver is characterized by slow progression to fibrosis and cirrhosis, end-stage liver diseases, and high risk of developing hepatocellular carcinoma (HCC) [3].

YKL40 (CHI3L1) is a member of the “mammalian chitinase-like proteins,” secreted by activated macrophages and neutrophils during inflammation in various tissues including liver, smooth muscle and cancer cells [4]. YKL40 is elevated in patients with chronic liver diseases that are characterized by inflammation and increased extra-cellular remodeling [5,6]. Although increased levels of YKL40 have been shown to be induced by tumor necrosis factor alpha (TNF α), the molecular mechanisms are not clearly identified [7]. TNF α , an inflammatory cytokine regulates gene expression in the nuclear factor of Kappa B (NFKB) signaling pathway [8]. Components of the mammalian NFKB family of transcription factors includes NFKB1 (P105/P50), NFKB2 (P100/P52), RelA (P65), RelB and c-Rel [9]. The NFKB component P65

is a multimeric DNA binding transcription factor involved in inflammatory and immune disorders especially autoimmune diseases and cancer [10]. NOTCH1 is one of the upstream regulator of NFKB complex and downregulation of NOTCH1 impairs its function [11,12]. It has been shown that NOTCH1 and TNF α regulate nuclear retention of NFKB [13,14]. CCAAT/enhancer-binding protein alpha (CEBP α) is a homodimeric DNA binding bZIP transcription factor that controls cell proliferation and differentiation [15]. CEBP α is differentially regulated in cases of HCC and targets expression of a wide range of genes and microRNAs (miRNA) involved in liver diseases [16,17].

miRNAs have been shown to play an important role in immune evasion, regulation of cell cycle and in cancer progression [18,19,20]. HCV infection results in modulation of miRNA particularly those that control viral particle entry and propagation, thus playing an important role in host immune evasion [21]. In this study we defined the molecular mechanisms of *YKL40* expression that involves HCV induced miRNA modulation and regulation by novel pathways including NOTCH1, NFKB and CEBP α .

Table 1. Patient Demographics.

Demographic	HCV	AH	NASH	Control
Number (n)	10	10	10	10
Age (mean, SD)	57±4	50±7	54±5	34±13
Gender M:F	6:4	5:5	7:3	5:5
Recipient Race (n)				
Caucasian	5	4	5	5
African American	5	5	5	5
Others		1		
Bilirubin (mg/dL)	1.9±0.4	1.5±0.3	1.8±0.6	0.9±0.8
AST (IU/ml)	90±34	110±40	74±30	25±10
ALT (IU/ml)	55±29	140±60	63±38	23±12
HCV Viral load (X10 ⁶ /mL)	1.4±0.3	n/a	n/a	n/a
HCV genotype				
1	4	n/a	n/a	n/a
%	21.5%	n/a	n/a	n/a
1a	4	n/a	n/a	n/a
%	30.8%	n/a	n/a	n/a
1b	2	n/a	n/a	n/a
%	15.4%	n/a	n/a	n/a

SD: Standard Deviation, HCV: Hepatitis C Virus, AH: Alcoholic Hepatitis, NASH: Non-Alcoholic Steatohepatitis, M: Male, F: Female, AST: Aspartate Amino Transferase, ALT: Alanine Amino Transferase.
doi:10.1371/journal.pone.0050826.t001

Materials and Methods

Patients

Liver biopsies were obtained from 10 chronic HCV patients, 10 alcoholic hepatitis patients, 10 non-alcoholic steatohepatitis patients and 10 normal donor livers (control) at the time of transplantation at Washington University Medical Center/Barnes-Jewish Hospital (Table 1). Patients with hepatitis B virus and/or HIV were excluded from the study. All of the human studies were approved by the human research protection committee at Washington University (protocol 201104075) and patients were enrolled after written informed consent was obtained.

Plasmids and Constructs

For *YKL40* luciferase constructs, the promoter regions were amplified from human genomic DNA (Zyagen, CA) by PCR using iProof High-Fidelity DNA Polymerase (Biorad, CA). PCR products were subcloned into pGL4.11 vector (Promega, WI) upstream of a luciferase gene using the NheI/EcoRV restriction sites. P65 and CEBP α were amplified from a human cDNA library (Stratagene, CA) and subcloned into pcDNA using the HindIII/NotI and HindIII/BamHI restriction sites, respectively. Hsa-miRNA-449a (SC400399) and control constructs were purchased from Origene, MD. *NOTCH1* (sc-36095), P65 (sc-29410) and control siRNA (sc-37007) were purchased from Santa Cruz Biotechnology, CA. Computational analysis of the promoter bound transcription factors was done using the Transcription Element Search System <http://www.cbil.upenn.edu/cgi-bin/tess/tess>. miRNA target analysis was done using <http://www.targets.org>.

miRNA and mRNA Expression Analysis

Total RNA was isolated from the liver biopsies or hepatocytes using the RNAaqueous kit (Ambion, NY). Expression level of miRNA-449a was determined using the TaqMan[®] MicroRNA

assays and TaqMan[®] Universal Master Mix II (Life technologies, NY) using predesigned primers. Quantitative PCR (qPCR) to analyze *YKL40* and *NOTCH1* was performed using a BioRad Real-Time PCR System with cycling conditions of 95°C for 10 min followed by 95°C for 15 sec and 60°C for 60 sec for a total of 40 cycles. Each TaqMan assay was run in triplicate. The $\Delta\Delta Ct$ value was calculated by normalizing the threshold (CT) values with *GAPDH* expression and respective gene expression in controls.

Primary Hepatocytes and HEPG2 Cell Line Transfection

Primary human hepatocytes were purchased from Life Technologies, New York and grown in 24 well plates in Williams Medium E supplemented with 5% FCS, 100 units/mL penicillin, 100 units/mL Amphotericin, 0.1% Albumin, 300 nM insulin, 2 mM L-glutamine and 0.1 nM Hydrocortisone. HEPG2 cells were grown in RPMI with 10% FBS, 1 mM sodium-pyruvate, 10 mM HEPES, 2 mM L-glutamine, and 100 units/mL penicillin/streptomycin. 20 ng/ml of TNF α (Sigma, St. Louis, MO) was added for 6 hours wherever indicated. The optimal concentration of TNF α was determined by dose-dependent analyses.

For transfection of hepatocytes and HEPG2 cells (ATCC), 0.2×10^5 cells were seeded into each well of a 24 well plate and grown for 24–48 hours. On the day of transfection, medium was changed and 500 ng of DNA was transfected using Lipofectamine[™] LTX and Plus Reagent (Invitrogen, NY). For siRNA delivery 0.1×10^5 cells were grown in each well of a 24 well plate for 24–48 hours in antibiotic free medium and 80 pico moles of siRNA were transfected using Lipofectamine[™] RNAiMAX (Invitrogen). Cells were harvested 48 hours post transfection and efficiency was measured by qPCR, immunostaining and western blot.

Western Blot and Immunofluorescence Microscopy

For localization of YKL40, NOTCH1 and P65, 50,000 HEPG2 cells were grown on coverslips in 24 well plates. Immunostaining was done as described before [22]. Briefly, cells were fixed with 4% paraformaldehyde and permeabilized with 0.1% Triton X-100. 2% normal goat serum in DPBS with 1% BSA, 0.1% Tween 20 was used for blocking and washing. Primary antibodies for western blot and Immunofluorescence used were goat anti-YKL40 (sc-31722), rabbit anti-NOTCH1 (sc-9170), mouse anti-CEBP α (sc-166258) and rabbit anti-P65 (sc-109). The secondary antibodies used were FITC-conjugated anti-mouse IgG (sc-2010), Rhodamine-conjugated anti-goat IgG (sc-3945) and Rhodamine-conjugated anti-rabbit IgG (sc-2492). The images were captured using an Eclipse 80i fluorescent microscope (Nikon, NY) and processed using Metamorph version 6.3r2 software (Molecular Devices, CA). Extraction of the nuclear and cytoplasmic fractions from the hepatocytes (1×10^6 cells) was done using NE-PER[®] Nuclear and Cytoplasmic Extraction Kit (Thermo Scientific, IL).

Luciferase Assay

Human primary hepatocytes (1×10^5) were transfected in 24 well plates as mentioned earlier with 1 μ g pGL4.11 luciferase reporter vector or pGL4.11 driven by the *YKL40* promoter or deletion constructs. For miRNA regulation studies the reporter construct was transfected in combination with 1 μ g of either control vector or vector expressing miRNA-449 precursor. For *NOTCH1* regulation studies the reporter construct was transfected in combination with 80 picomoles of either non specific siRNA or siRNA specific for *NOTCH1*. For transcription factor studies the reporter constructs were transfected in combination with 2 μ g of empty pcDNA3 vector, or pcDNA3 expressing P65 or CEBP α or

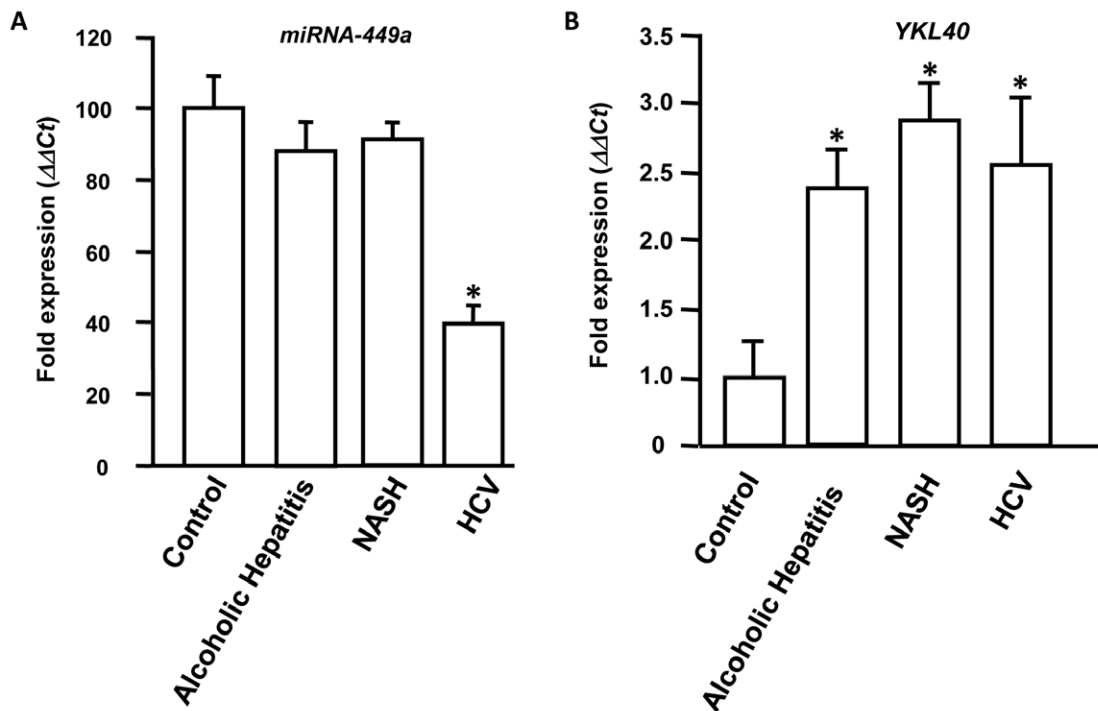


Figure 1. miRNA-449a is downregulated in HCV patients and YKL40 is upregulated in patients with hepatic fibrosis. Total RNA was isolated from liver biopsies obtained from 10 chronic HCV patients, 10 alcoholic hepatitis patients, 10 non-alcoholic steatohepatitis (NASH) patients and 10 normal donor livers (control). Expression of miRNA-449a (1A) and YKL40 (1B) were determined by Q-PCR. The $\Delta\Delta Ct$ value was calculated by normalizing the threshold (CT) values with GAPDH expression and miRNA-449a (1A) or YKL40 (1B) expression respectively in controls. The * represents p value < 0.01 obtained by a two-tailed t test. Error bars represent Standard Deviations (SD) calculated from three independent experiments.

doi:10.1371/journal.pone.0050826.g001

both. 20 ng/ml of TNF α was added to the medium 6 hours before harvesting. To control for efficiency of transfection, 0.1 μ g of pRL-TK (Promega, Madison, WI), which expresses Renilla luciferase was included. Luciferase activity was measured 48 h after electroporation using the Dual Luciferase Reporter Assay System (Promega, Madison, WI) and the results were normalized to Renilla luciferase.

Co-immunoprecipitation

Immunoprecipitation of P65 with CEBP α or the reverse immunoprecipitation in TNF α treated hepatocytes (1×10^6) were carried out as described by Sarma et al [22]. Briefly, cells were washed with DPBS, and lysed with 0.5 ml of lysis buffer (10 mM Tris-HCl, pH 7.5, 0.4 M NaCl, 1% Nonidet P-40, 0.4% Triton X-100, 0.2% sodium deoxycholate, 1 mM EDTA, protease inhibitors (PI), 1 mM PMSF). Diluted with 0.5 ml buffer containing 10 mM Tris-HCl, pH 7.5, 1 mM EDTA, PI, 1 mM PMSF and centrifuged at $17,000 \times g$ for 30 min. 1 μ g normal mouse/rabbit IgG or mouse anti-CEBP α or rabbit anti-P65 was used to immunoprecipitate the complexes from the supernatant. After overnight incubation with the antibodies 30 μ l of Protein G beads were added to lysates and incubated for another 1 hour. Beads were washed with 700 μ l of wash buffer (10 mM Tris-HCl, pH 7.5, 0.2 M NaCl, 0.5% Nonidet P-40, 0.2% Triton X-100, 0.1% sodium deoxycholate, 1 mM EDTA, PI, 1 mM PMSF) 3 min each for 5 times and once with cold DPBS by centrifugation at $1,800 \times g$ for 3 min at 4°C. Immunocomplexes were eluted by boiling with 30 μ l of 2X SDS buffer (0.1 M Tris-HCl, pH 6.8, 3.5% SDS, 10% glycerol, 2 mM DTT, 0.004% bromophenol blue) for 10 min and subjected to SDS-PAGE (4–20% gel). P65 or

CEBP α were detected with a rabbit anti-P65 or a mouse anti-CEBP α respectively.

Chromatin Immunoprecipitation

Chromatin Immunoprecipitation was carried out with ChIP-ITTM Express (Active Motif, Carlsbad, CA). Briefly, hepatocytes (1×10^6) were crosslinked with 1% formaldehyde and quenched with 0.375 M glycine. Nuclei were isolated and sonicated in 350 μ l of shearing buffer to prepare chromatin extracts. 1 μ g of antibodies for control IgG, P65 or CEBP α were added to 60 μ l of sheared chromatin along with Protein G Magnetic Beads. Antibody-lysate mix was washed and DNA was eluted according to the instructions. YKL40 promoter regions were amplified by PCR.

Results

miRNA-449a is Downregulated in HCV Patients

A genomewide miRNA analysis in liver biopsies obtained from chronic HCV infected patients demonstrated a distinct expression profile when compared to the normal liver. Particularly, a significant downregulation of microRNA-449a was observed in the HCV infected livers.

To analyze the specific role of miRNA-449a following HCV infection, biopsies were obtained from 10 chronic HCV patients, 10 alcoholic hepatitis patients, 10 non-alcoholic Steatohepatitis (NASH) patients and 10 control normal donor livers at the time of liver transplant. Total RNA was isolated from the liver biopsies and expression level of miRNA-449a was determined by qPCR using specific primers and the results were normalized to GAPDH

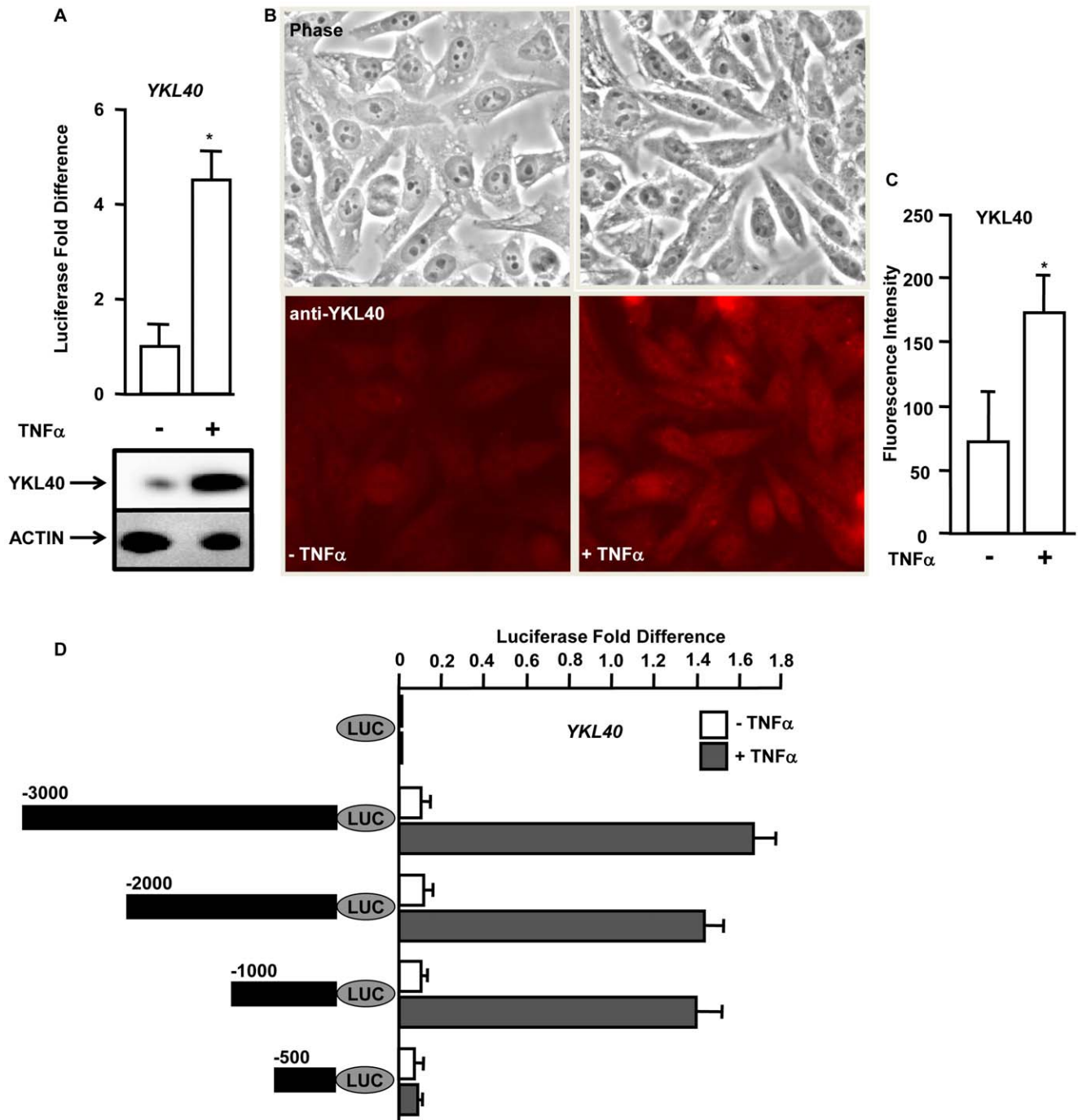


Figure 2. TNF α regulates the expression of YKL40 at the transcriptional level. A. (Upper panel) Hepatocytes were transfected with an -3000 bp YKL40-promoter driven reporter construct with (+) or without (-) TNF α . Firefly luciferase activity was measured 48 hours after transfection and normalized to a Renilla luciferase internal control. The numbers represent fold-change over control (average of three independent experiments); error bars represent SD. The * represents p value < 0.05 obtained by a two-tailed t test. (Lower panel): hepatocytes from 2A were immunoblotted with anti-YKL40 with (+) or without (-) TNF α . ACTIN was used as the loading control. B. HEPG2 cells were immunostained with anti-YKL40 antibody without (-) or with (+) TNF α . C. Quantification of the YKL40 immunostaining signal in HEPG2 cells (1B). The numbers represent the average fluorescence intensity of YKL40 (n = 100). D. Essential regions in the YKL40 promoter required for TNF α mediated expression. Hepatocytes were transfected with luciferase reporters driven by deletion constructs of YKL40 promoter (-3000 bp, -2000 bp, -1000 bp, -500 bp, filled black bars on left) construct with (+) or without (-) TNF α . Firefly luciferase activity was measured 48 hours after transfection and normalized to a Renilla luciferase internal control. The luciferase activity was normalized to the control empty luciferase vector and the numbers represent fold-change over control (average of three independent experiments); error bars represent SD calculated from three independent experiments. doi:10.1371/journal.pone.0050826.g002

expression. Expression analysis demonstrated that miRNA-449a is downregulated more than two fold in livers obtained from HCV

patients whereas no significant differences in the expression was observed in alcoholic hepatitis patients, NASH patients and

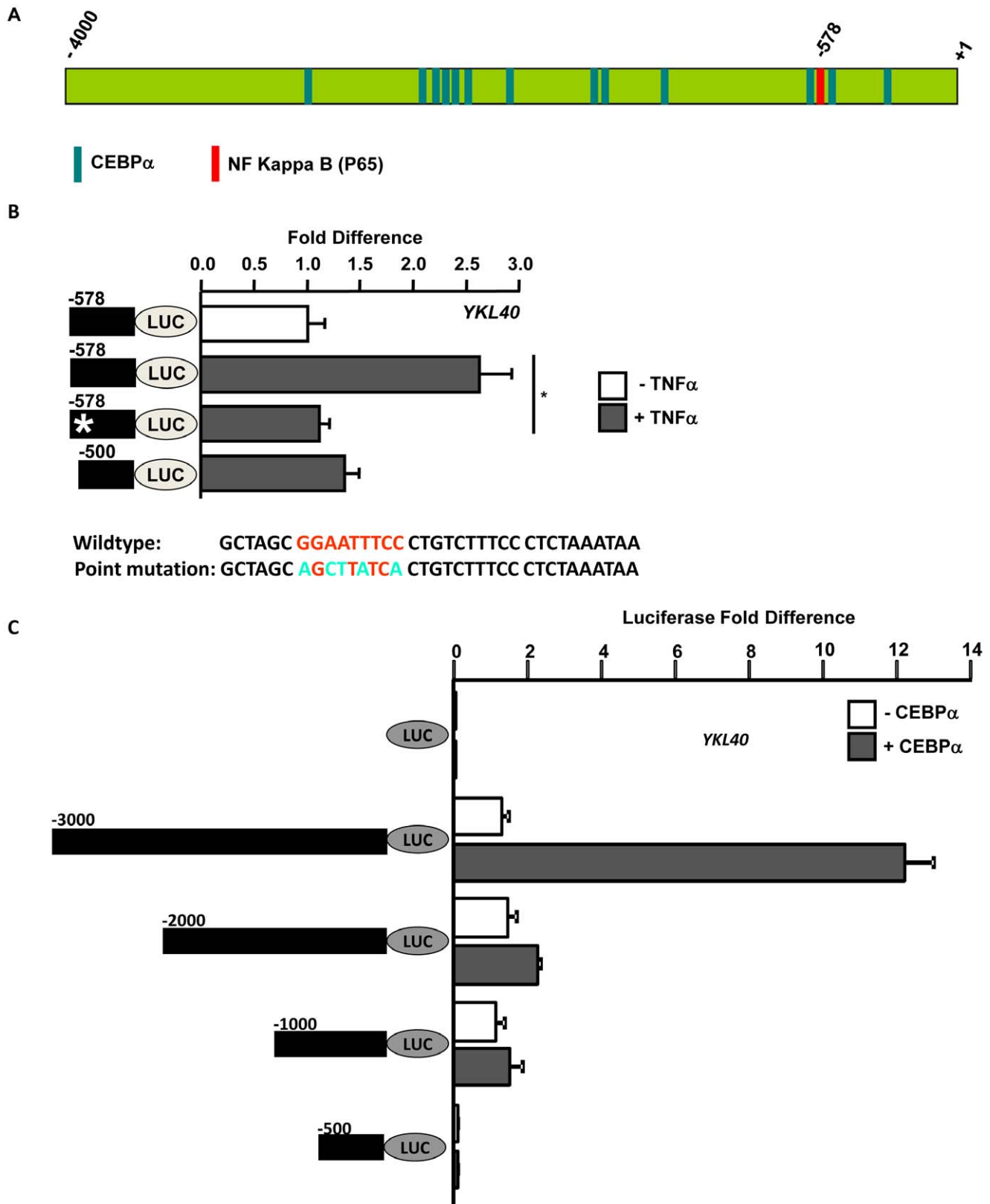


Figure 3. Transcription factors P65 and CEBP α regulate expression of YKL40. A. Computational prediction of transcription factors binding to the YKL40 promoter. Computational analysis of -4000 bp upstream of the open reading frame using the Transcription Element Search System (TESS). The bars represent the predicted consensus binding sites in the DNA for transcription factors P65 and CEBP α . B. Mutation of NFKB/P65 binding site inhibits TNF α mediated YKL40 induction. Hepatocytes were transfected with luciferase reporters driven by deletion constructs of YKL40 promoter -578 bp wildtype, -578 bp P65 binding site mutated (*) and -500 bp wildtype (P65 site deleted), filled black bars on left) construct with (+) or without (-) TNF α . Firefly luciferase activity was measured 48 hours after transfection and normalized to a Renilla luciferase internal control. The

numbers represent fold-change over the -578 wildtype construct without TNF α treatment (average of three independent experiments); error bars represent SD. The P65 binding site mutation is shown in the lower panel. The ^{*} represents p value <0.05 obtained by a two-tailed t test. C. CEBP α in an upstream transcription factor to activate *YKL40* expression. Hepatocytes were transfected with luciferase reporters driven by deletion constructs of *YKL40* promoter (-3000 bp, -2000 bp, -1000 bp, -500 bp, filled black bars on left) along with an empty vector or vector expressing CEBP α and treated with TNF α . Firefly luciferase activity was measured 48 hours after transfection and normalized to a Renilla luciferase internal control. The numbers represent fold-change over the control empty luciferase vector (average of three independent experiments); error bars represent SD. doi:10.1371/journal.pone.0050826.g003

normal livers (Figure 1A). This suggests that miRNA-449a is specifically downregulated in patients with liver diseases following HCV infection.

YKL40 is Upregulated in HCV Patients with Fibrosis

To determine the expression level of *YKL40* in liver diseases, biopsies were obtained from 10 chronic HCV patients, 10 alcoholic hepatitis patients, 10 NASH patients and 10 control normal donor livers at the time of liver transplant. Total RNA was isolated from the liver biopsies and expression level of *YKL40* was determined by qPCR using specific primers and the results were normalized to *GAPDH* expression. Expression analysis showed that *YKL40* to be upregulated in alcoholic hepatitis patients (2.4 fold), NASH patients (2.9 fold) and HCV patients (2.6 fold) compared to normals (Figure 1B). These results demonstrate that *YKL40* is elevated in patients with chronic liver diseases which are accompanied by inflammation.

TNF α Regulates the Expression of *YKL40* at the Transcriptional Level

We and others have shown that *YKL40* expression is elevated in patients with chronic liver diseases accompanied by inflammation [5,6]. *In vitro* studies have shown that inflammatory cytokines such as TNF α have the ability to induce expression of *YKL40* [7]. To study the molecular mechanisms of TNF α mediated regulation of *YKL40*, -3000 base pairs (bp) of the human *YKL40* promoter was cloned upstream of a luciferase reporter gene and the construct was introduced into human hepatocytes. The cells were treated either with or without 20 ng/ml TNF α for 6 hours and luciferase activity was measured. More than four fold increase in the *YKL40* promoter activity was observed in cells treated with TNF α compared to untreated (Figure 2A, upper panel). Further, western blot analysis showed increased expression of YKL40 in TNF α treated cells (Figure 2A, lower panel). This reporter gene analysis suggests that TNF α regulates the expression of *YKL40* through modulation of upstream transcriptional complexes that interact with the *YKL40* promoter.

To further demonstrate that TNF α induces expression of *YKL40*, human HEPG2 cells were cultured and treated with TNF α . Immunostaining of the HEPG2 cells with anti-YKL40 showed a more than 2 fold increase in expression of YKL40 in the cells treated with TNF α compared to untreated cells (Figures 2B and 2C).

Reporter Analysis Identified Essential Regions in the *YKL40* Promoter Required for TNF α Regulated Expression of YKL40

Since TNF α regulated the expression of *YKL40* at the transcriptional level we hypothesized the possible interaction of TNF α with upstream regulatory complexes of the *YKL40* gene. To identify the essential regions for TNF α mediated expression deletion mutants of the *YKL40* promoter regions were cloned upstream of a luciferase reporter gene. Sequential deletion mutants of the *YKL40* promoter region (Figure 2D, black filled bars on the left) were introduced into hepatocytes. The cells were treated with or without TNF α and the luciferase activity was

measured. Significant increases (>10 fold) in the expression from the *YKL40* promoter deletion constructs were observed in the cells treated with TNF α compared to untreated (Figure 2D). However, deletion of the -1000 to -500 bp region of the *YKL40* promoter impaired TNF α mediated transcriptional induction. This indicates that this region (-1000 to -500 bp) contains binding sites for transcriptional regulatory elements on the *YKL40* promoter.

Computational Prediction of Transcription Factors Regulating *YKL40* Expression

In order to identify transcription factors that regulate the expression of *YKL40* a computational analysis of -4000 bp upstream of the open reading frame was done using the transcription element search system. The program predicted consensus binding sites in the DNA for several transcription factors that included NF κ B subunit P65 and CEBP α (Figure 3A). The software predicted a consensus binding site for p65 (GGAATTTCC) at -578 bp position at the promoter. Similarly several DNA binding sites for CEBP α (CCAAT) was also predicted throughout the *YKL40* promoter. Most of the CEBP α binding sites were concentrated in the -3000 to -2000 bp region of the promoter. Interestingly, two CEBP α binding sites were identified in close proximity to the P65 DNA binding site on the promoter (Figure 3A) suggesting that these two transcription factors may bind to the *YKL40* promoter by forming a transcriptional regulatory complex.

Mutation of NF κ B (P65) Binding Site Inhibits TNF α Mediated *YKL40* Induction

Computational analysis predicted a putative binding site for NF κ B subunit P65 at -578 bp position of the human *YKL40* promoter. Further the *YKL40* promoter analysis using the deletion constructs identified -1000 to -500 bp region to be essential for TNF α mediated induction of *YKL40* in hepatocytes. To test whether P65 binding plays a role in TNF α mediated upregulation of *YKL40* promoter a -578 bp wildtype luciferase reporter construct, a -578 bp construct with point mutations in the P65 binding site (wildtype: GGAATTTCC, point mutation: AGCT-TATCA) and a -500 bp construct with P65 binding site deleted were prepared. Hepatocytes were transfected with these three reporter constructs and cells were treated either with or without TNF α and Luciferase activity was measured. As expected the wildtype -578 bp promoter construct with an intact P65 binding site showed two fold increase in transcriptional activity in the presence of TNF α (Figure 3B). However, point mutation in the P65 binding site or deletion of the P65 binding site (-500 bp) completely abolished TNF α mediated induction of *YKL40* (Figure 3B). Further, we demonstrated that siRNA mediated knockdown of P65 resulted in impairment of transcriptional activation by the *YKL40* promoter in TNF α treated cells.

CEBP α in an Upstream Transcription Factor which Activate *YKL40* Expression

Computational analysis identified CEBP α as a putative DNA binding factor for transcriptional regulation of *YKL40*. To test whether CEBP α regulates *YKL40* expression an empty vector or

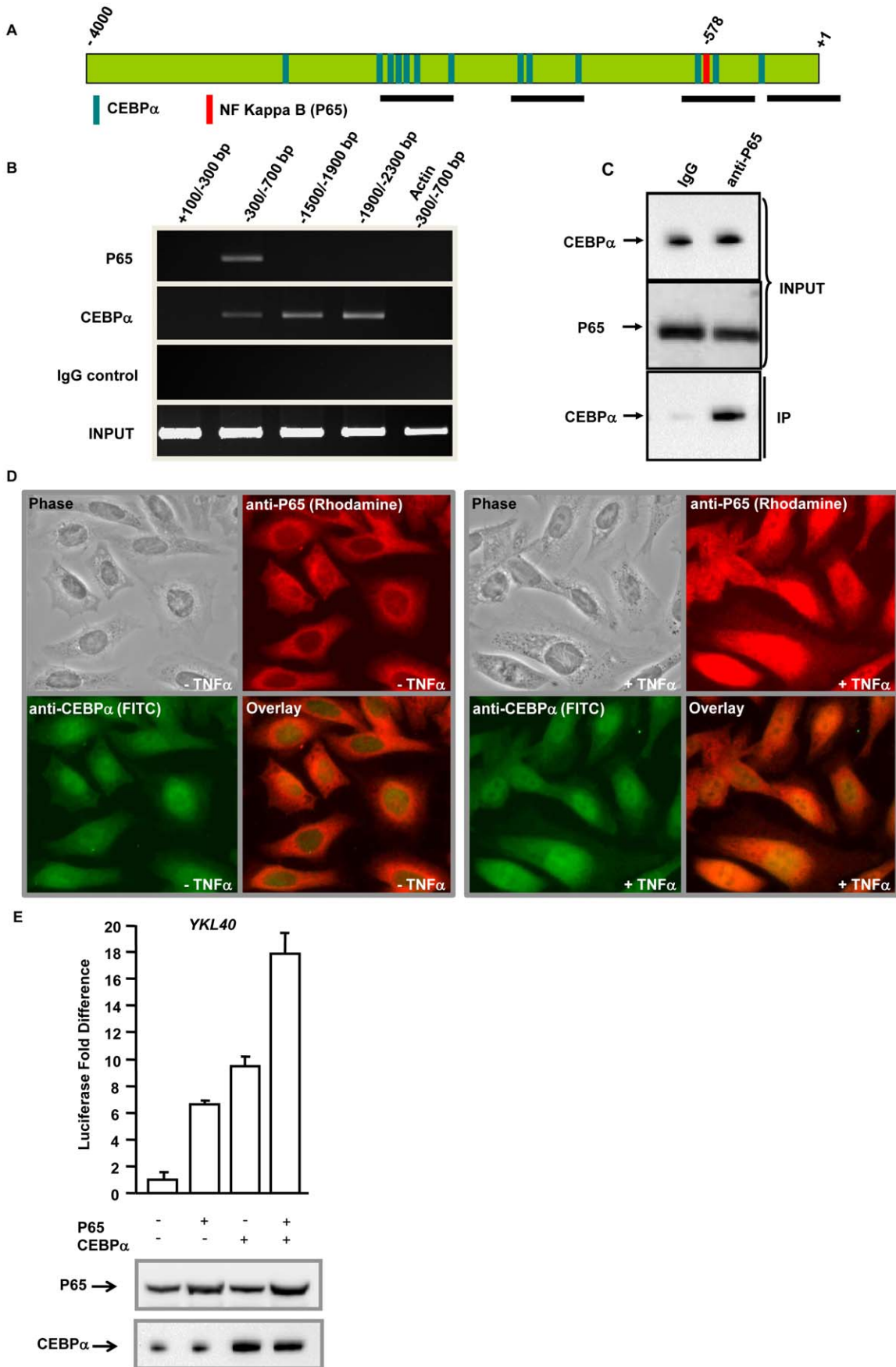


Figure 4. CEBP α interacts with NFKB/P65 to bind YKL40 promoter and cooperates to activate transcription in hepatocytes. A. YKL40 promoter showing binding sites for P65 and CEBP α . The black horizontal bars represent regions amplified by the PCR primers. B. Chromatin was immunoprecipitated with anti-P65 or anti-CEBP α or isotype control IgG from hepatocytes. Segments of the YKL40 promoter (indicated in 4A) were amplified by PCR. The first three lanes show immunoprecipitated chromatin (IP) and the fourth lane show input chromatin (Input). ACTIN promoter amplification is shown as the negative control. C. Co-immunoprecipitation of P65 with CEBP α in hepatocytes. Whole cell lysates were subjected to immunoprecipitation with either rabbit IgG or anti-P65. CEBP α in the cell lysates (Input) and immunoprecipitated complexes (IP) was detected by immunoblotting with anti-CEBP α . P65 was detected by immunoblotting with anti-P65. D. HEPG2 cells were treated with (+) or without (–) TNF α and co-immunostained with anti-CEBP α and anti-P65. E. Hepatocytes were transfected with a luciferase construct driven by the –3000 bp YKL40 promoter in addition to the control vector or vector expressing P65 or CEBP α or both. Firefly luciferase activity was measured 48 hours after transfection and normalized to a Renilla luciferase internal control. The numbers represent fold-change over the control empty vector (average of three independent experiments); error bars represent SD. Bottom panel, expression of P65 and CEBP α was verified by immunoblotting with anti-P65 and anti-CEBP α respectively.
doi:10.1371/journal.pone.0050826.g004

a vector expressing CEBP α was overexpressed in hepatocytes along with deletion mutants of the YKL40 promoter cloned upstream of a luciferase reporter gene. The deletion mutants included –3000 bp, –2000 bp, –1000 bp and –500 bp of the YKL40 promoter region (Figure 3C, black filled bars on the left) and the luciferase activity was measured after the cells were treated with TNF α for 6 hours. Significant increases (>9 fold) in the YKL40 expression from the –3000 bp promoter construct was noted when CEBP α was overexpressed compared to control empty vector (Figure 3C). However, deletion of the –3000 bp to –2000 bp region of the YKL40 promoter impaired CEBP α mediated transcriptional induction of YKL40 as that region contained several putative CEBP α binding sites as shown on our computational analysis (Figure 3A).

CEBP α Interacts with NFKB/P65 to Bind YKL40 Promoter and Cooperates to Activate Transcription in Hepatocytes

Reporter analysis demonstrated that both P65 and CEBP α regulate expression from the YKL40 promoter. To test whether P65 and CEBP α interact and bind to adjacent consensus sites present on the YKL40 promoter a chromatin immunoprecipitation analysis was done. TNF α treated hepatocytes were fixed with formaldehyde and chromatin extracts were prepared. The DNA-protein complexes were immunoprecipitated with anti-P65 or anti-CEBP α or isotype control IgGs. Chromatin fragments were isolated from the immunoprecipitated DNA-protein complexes and subjected to PCR amplification using primers specific for YKL40 promoter regions as shown in Figure 4A. The PCR products were resolved on agarose gel. Chromatin immunoprecipitation analysis showed that both P65 and CEBP α bind to the YKL40 promoter (Figure 4B). P65 binds to the –300 bp to –700 bp region of the YKL40 whereas no binding was observed with other regions of the promoter. This region encompasses the P65 binding site at –578 bp position. CEBP α showed binding to several regions of the YKL40 promoter where maximum band intensity was seen at –1900 bp to –2300 bp region that encompasses most of the CEBP α binding sites. Immunoprecipitation with isotype IgGs did not enrich any of these YKL40 promoter regions demonstrating the specificity for P65 or CEBP α . No amplification of DNA was observed in PCR reactions performed with primers specific for ACTIN promoter.

Binding of both CEBP α and P65 to the YKL40 promoter in adjacent DNA binding sites suggests the possibility that they interact with each other. To test this, crude lysates from TNF α treated hepatocytes were prepared and subjected to immunoprecipitation with either isotype control IgG or anti-P65 followed by immunoblotting with anti-CEBP α . CEBP α was co-immunoprecipitated with endogenous P65 whereas no CEBP α was observed with the control IgG (Figure 4C). To confirm the interaction a reverse co-immunoprecipitation was done by immunoprecipitation with either isotype control IgG or anti-CEBP α followed by

immunoblotting with anti-P65 (Figure S1). To further demonstrate the interaction between P65 and CEBP α , HEPG2 cells were treated with or without TNF α and co-immunostained with anti-CEBP α and anti-P65. CEBP α primarily localized to the nucleus in both TNF α treated and untreated cells. P65 remained exclusively cytoplasmic in the untreated cells with little to no nuclear localization. In the TNF α treated cells, a significant amount of P65 translocated into the nucleus and co-localized with CEBP α (Figure 4D).

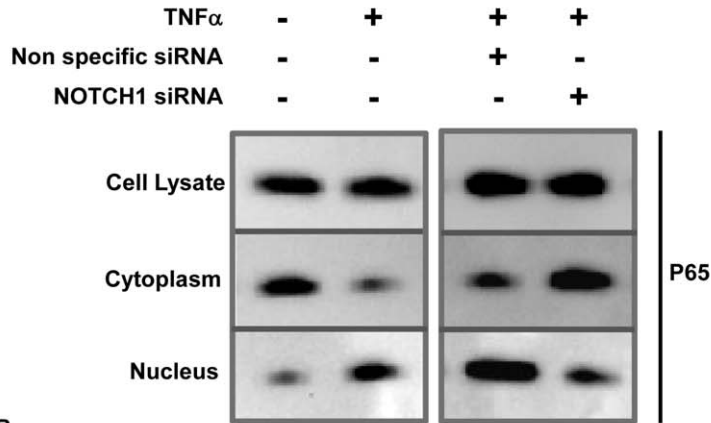
Immunoprecipitation and co-localization analyses indicated that both P65 and CEBP α interact with each other and bind to their consensus sites on the YKL40 promoter. To determine their role in transcriptional regulation from the YKL40 promoter, hepatocytes were co-transfected with a luciferase reporter construct driven by the YKL40 promoter (–3000 bp) with P65 or CEBP α or both. Overexpression of both P65 and CEBP α resulted in significant increase in transcriptional activation of the reporter construct compared to either alone (Figure 4E, upper panel). Immunoblotting of the cell lysates with anti-P65 and anti-CEBP α confirmed the elevated expression levels of these factors compared to endogenous levels (Figure 4E, lower panel). This demonstrates that CEBP α cooperates with NFKB to regulate expression from the YKL40 promoter.

NOTCH1 Regulates Nuclear Retention of NFKB/P65 in Response to TNF α

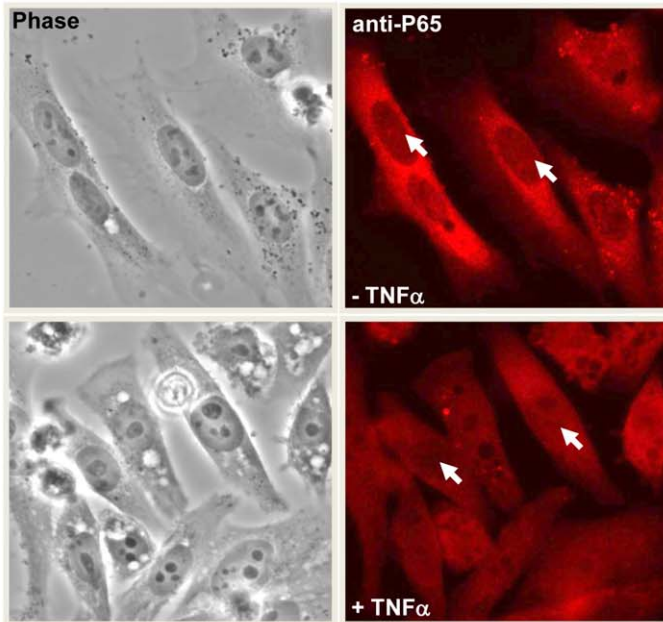
Results presented clearly demonstrates that TNF α mediated regulation of YKL40 is dependent on the NFKB subunit P65. To demonstrate nuclear translocation of P65 in response to TNF α in hepatocytes, cells were treated with or without TNF α and cytoplasmic and nuclear extracts were prepared. Whole cell lysates, the cytoplasmic fraction and the nuclear fraction were subjected to immunoblotting with anti-P65. The expression of P65 was not affected by TNF α as no difference was observed in the whole cell lysate (Figure 5A, left panel). However, significant cytoplasmic exclusion and nuclear enrichment of P65 was observed in TNF α treated cells compared to untreated cells. One of the essential upstream regulators of NFKB complex is NOTCH1 [11,12]. To analyze the role of NOTCH1, an upstream factor required for TNF α mediated nuclear localization of P65, and its functionality in facilitating downstream gene regulation, hepatocytes were transfected either with scrambled siRNA or siRNA specific for human NOTCH1 and subjected to TNF α treatment. The siRNA mediated knockdown of NOTCH1 was confirmed by immunoblotting with anti-Notch1 (Figure S2A). Immunoblot using anti-P65 demonstrated that knockdown of NOTCH1 resulted in impairment of TNF α mediated cytoplasmic exclusion and nuclear translocation of P65 (Figure 5A, right panel).

To further demonstrate that NOTCH1 is required for TNF α mediated translocation of P65, HEPG2 cells were treated with or

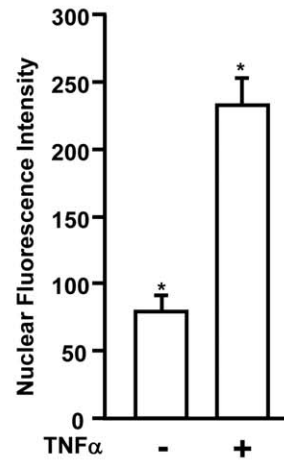
A



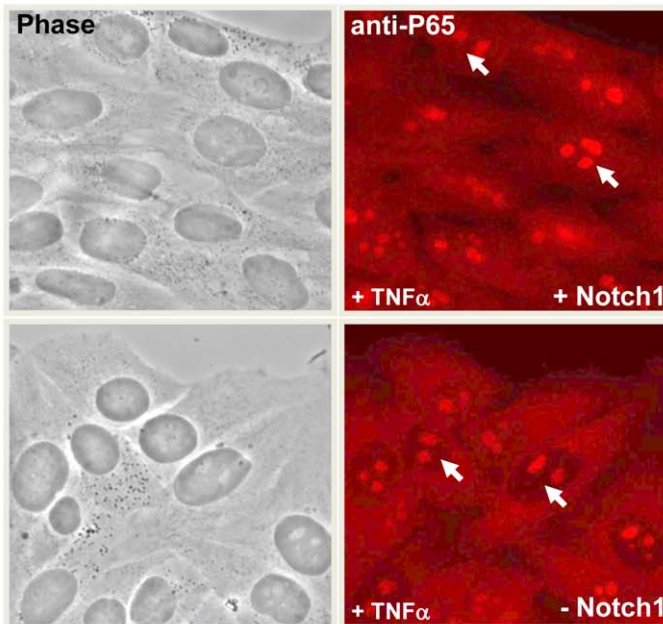
B



C



D



E

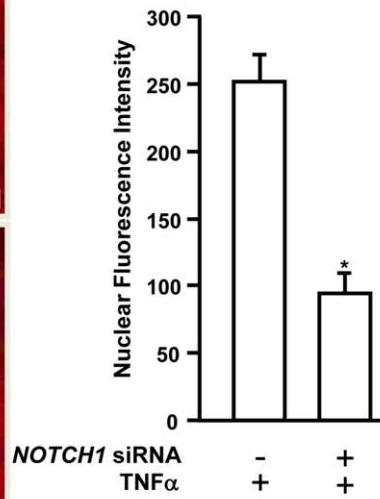


Figure 5. Notch1 regulates nuclear retention of NFkB/P65 in response to TNF α . A. (Right panel) Hepatocytes were treated with (+) or without (-) TNF α and cytoplasmic and nuclear fractions were extracted. (Left panel) hepatocytes were transfected with either non-specific siRNA or siRNA specific for NOTCH1 and treated with TNF α and cytoplasmic and nuclear fractions were extracted. Whole cell lysates, cytoplasmic and nuclear extracts were subjected to immunoblotting with anti-P65. B. HEPG2 cells were treated with (+) or without (-) TNF α and immunostained with anti-P65. The arrows indicate nuclear localization of P65. C. Quantification of the P65 immunostaining signal in HEPG2 cells (5B). The numbers represent the average fluorescence intensity of P65 (n = 100). D. HEPG2 cells were transfected with either non-specific siRNA or siRNA specific for NOTCH1 and treated with TNF α . The arrows indicate nuclear localization of P65. E. Quantification of the P65 immunostaining signal in HEPG2 cells (5D). The numbers represent the average fluorescence intensity of P65 (n = 100). The "*" represents p value < 0.05 obtained by a two-tailed t test. doi:10.1371/journal.pone.0050826.g005

without TNF α and probed for P65 localization by immunostaining with anti-P65 (Figure 5B). In the untreated cells P65 remained

exclusively cytoplasmic with little to no nuclear localization observed. In the TNF α treated cells, a significant amount of P65

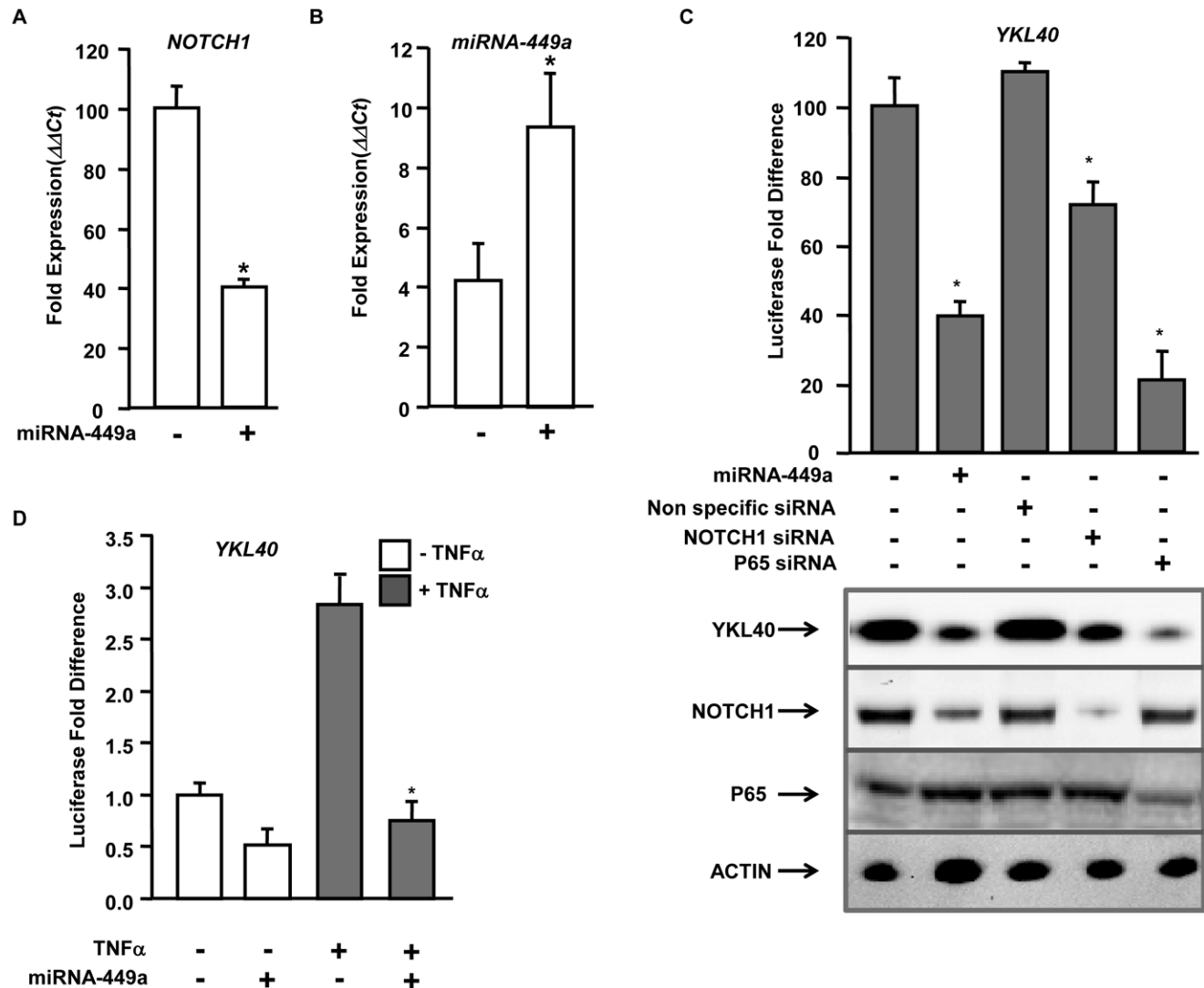


Figure 6. microRNA 449a regulates YKL40 expression by targeting NOTCH1 for silencing. A & B. Hepatocytes were transfected with an empty vector (-) or vector expressing miRNA-449a (+) and expression of NOTCH1 (6A) and miRNA-449a (6B) were determined by Q-PCR. The $\Delta\Delta Ct$ value was calculated by normalizing the threshold (CT) values with GAPDH and expression of NOTCH1 and miRNA-449a respectively in controls. The "*" represents p value < 0.05 obtained by a two-tailed t test. C. (Upper panel) hepatocytes were transfected with a luciferase construct driven by the YKL40 promoter in addition to the control vector or vector expressing miRNA-449a or non-specific siRNA or siRNA specific for NOTCH1 or siRNA specific for P65 in the presence of TNF α . Firefly luciferase activity was measured 48 hours after transfection and normalized to a Renilla luciferase internal control. The numbers represent fold-change over the control vector (average of three independent experiments); error bars represent SD. (Lower panel) Downregulation of YKL40, NOTCH1 and P65 is verified by immunoblotting with anti-YKL40 or anti-NOTCH1 or anti-P65 respectively. ACTIN is shown as the loading control. D. Hepatocytes were transfected with a luciferase construct driven by the YKL40 promoter in addition to the control vector or vector expressing miRNA-449a construct with (+) or without (-) TNF α . Firefly luciferase activity was measured 48 hours after transfection and normalized to a Renilla luciferase internal control. The numbers represent fold-change over the control vector without TNF α (average of three independent experiments); error bars represent SD. The "*" represents p value < 0.01 obtained by a two-tailed t test. doi:10.1371/journal.pone.0050826.g006

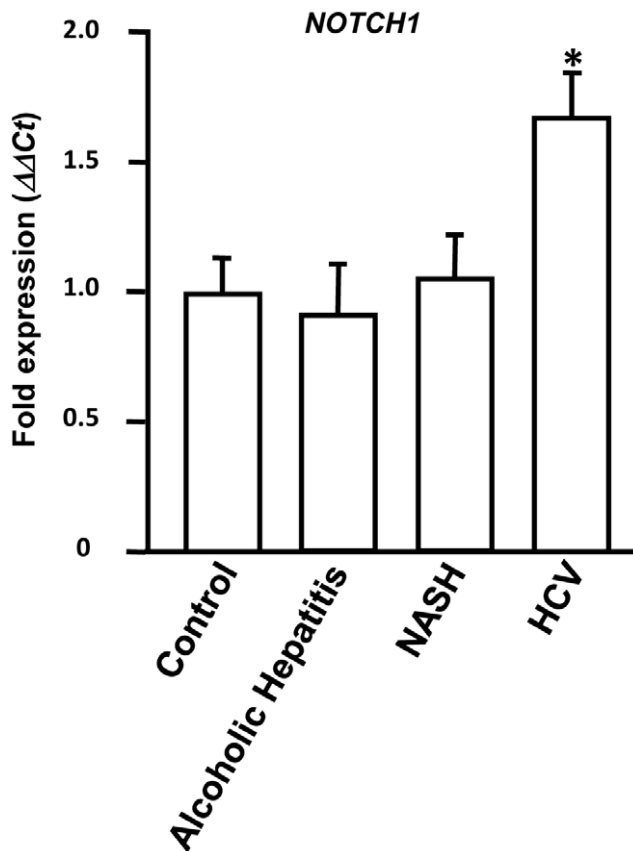


Figure 7. NOTCH1 expression is upregulated in HCV patients. Total RNA was isolated from liver biopsies obtained from 10 chronic HCV patients, 10 alcoholic hepatitis patients, 10 NASH patients and 10 normal donor livers (control). Expression of *NOTCH1* was determined by Q-PCR. The $\Delta\Delta Ct$ value was calculated by normalizing the threshold (CT) values with *GAPDH* expression and expression of *NOTCH1* in controls. The '*' represents p value < 0.01 obtained by a two-tailed t test. Error bars represent SD.
doi:10.1371/journal.pone.0050826.g007

translocated into the nucleus and quantification showed more than three fold nuclear abundance of P65 compared to the untreated cells (Figure 5C). Next, the HEPG2 cells were transfected with either scrambled siRNA or siRNA specific for human *NOTCH1* and subjected to $TNF\alpha$ treatment. Immunostaining with anti-Notch1 showed more than four fold knockdown of *NOTCH1* by siRNA (Figure S2B, C). Knockdown of *NOTCH1* resulted in impairment of $TNF\alpha$ mediated nuclear translocation of P65 by two fold (Figures 5D and E). $TNF\alpha$ mediated nuclear localization of P65 in cells transfected with scrambled siRNA was not affected. This finding indicates that *NOTCH1* acts as an upstream regulatory factor and controls $TNF\alpha$ mediated nuclear translocation of P65.

miRNA-449a Regulates *YKL40* Expression by Modulating *NOTCH1* Expression

Genomewide microarray analysis in our laboratory followed by miRNA gene expression analysis showed that miRNA-449a is downregulated more than two fold in HCV patients compared to non-HCV liver diseases and normals (Figure 1A). Computational target prediction of miRNA-449a using Targetscan (Targetscan.org) identified *NOTCH1* to be a putative target for translational silencing. To test this, hepatocytes were transfected with either

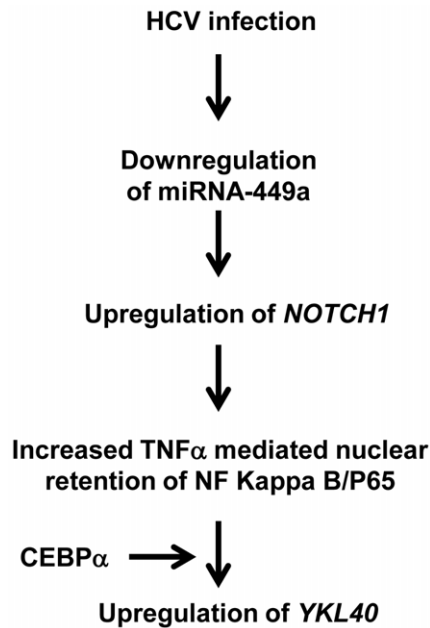


Figure 8. Schematic representation of HCV mediated role of miRNA-449a in *YKL40* expression. HCV infection results in downregulation of miRNA-449a that leads to upregulation of *NOTCH1* eventually results in nuclear stabilization of P65. P65 upregulates *YKL40* expression in co-operation with CEBP α in response to $TNF\alpha$.
doi:10.1371/journal.pone.0050826.g008

empty vector of vector expressing miRNA-449a and expression of both miRNA-449a and *NOTCH1* were determined by qPCR. The results were normalized to *GAPDH* expression. Increased expression of miRNA-449a resulted in more than two fold downregulation of *NOTCH1* (Figure 6A and B).

Earlier we have shown that NF κ B component P65, a protein regulated by *NOTCH1*, activates *YKL40* expression through sequence specific promoter interaction (Figures 3 and 4). It is likely that downregulation of miRNA-449a in HCV infected patients (Figure 1A) results in activation of *NOTCH1*/NF κ B signaling that leads to upregulation of *YKL40* expression. To test whether miRNA-449a regulates *YKL40* expression, hepatocytes were transfected with either a control vector or vector expressing miRNA-449a along with an *YKL40* promoter-driven luciferase reporter construct. In $TNF\alpha$ treated cells expression of *YKL40* is reduced by more than two fold in the presence of miRNA-449a (Figure 6C, upper panel). qPCR analysis also showed downregulation of *YKL40* by increased expression of miRNA-449a (Figure S3).

Since, computational target analysis did not identify *YKL40* to be a direct target for miRNA-449a; results obtained from promoter based reporter analysis suggest that miRNA-449a regulates the expression of *YKL40* by silencing components of upstream transcriptional regulatory complexes such as *NOTCH1*/NF κ B. To demonstrate that downregulation of *YKL40* expression by miRNA-449a is mediated by silencing *NOTCH1*, hepatocytes were transfected with either scrambled siRNA or siRNA specific for *NOTCH1* along with an *YKL40*-driven luciferase reporter construct and cells were treated with $TNF\alpha$. siRNA mediated knockdown of *NOTCH1* impaired expression from the *YKL40* promoter (Figure 6C, upper panel). We have demonstrated that nuclear P65, regulated by *NOTCH1*, activates *YKL40* expression in response to $TNF\alpha$. siRNA mediated knockdown of P65 also impaired expression from the *YKL40*

promoter (Figure 6C, upper panel). Western blot analysis using anti-YKL40 showed downregulation of *YKL40* by expression of miRNA-449a or siRNA mediated knockdown of *NOTCH1* or P65 in hepatocytes (Figure 6C, lower panels). qPCR analysis also confirmed downregulation of *YKL40* by miRNA-449a (Figure S3). Immunoblot analysis using anti-NOTCH1 demonstrated that expression of miRNA-449a resulted in downregulation of NOTCH1. Since, P65 is a downstream factor for NOTCH1, knockdown of P65 did not affect its expression (Figure 6C, lower panels). This suggests that miRNA-449a regulates expression of *YKL40* by modulating the NOTCH1 signaling pathway.

To further determine if TNF α mediated activation of *YKL40* is regulated by miRNA-449a, hepatocytes were transfected with either a control vector or vector expressing miRNA-449a along with an *YKL40*-driven luciferase reporter construct (–3000 bp) and cells were treated with or without TNF α . In the cells expressing the empty vector, TNF α induced expression from the *YKL40* promoter (Figure 6D). However, in presence of miRNA-449a this TNF α mediated upregulation of *YKL40* was impaired.

NOTCH1 Expression is Upregulated in HCV Patients

To determine whether downregulation of miRNA-449a in HCV infection is accompanied by upregulation of its target *NOTCH1*, biopsies were obtained from 10 chronic HCV patients, 10 alcoholic hepatitis patients, 10 NASH patients and 10 control normal donor livers at the time of liver transplant. Total RNA isolation followed by qPCR demonstrated *NOTCH1* to be significantly upregulated in livers obtained from HCV patients. However, no significant difference in the expression of *NOTCH1* was observed in alcoholic hepatitis patients, NASH patients and normal livers (Figure 7). Based on our *in-vitro* results obtained with hepatocytes, upregulation of *NOTCH1* and *YKL40* (Figure 1) in HCV patients can be attributed to downregulation of miRNA-449a.

Discussion

YKL40, a member of the mammalian chitinase-like protein, has been shown to be elevated in patients with chronic liver diseases with fibrosis and cirrhosis (Figure 1) [5,6]. In chronic liver disease patients, YKL40 expression has been shown to have a strong correlation with degree of fibrosis progression, extracellular matrix (ECM) synthesis, and serves an early indicator of liver fibrosis [23,24]. In HCC patients, YKL40 expression is highly elevated in both serum and liver tissue [25]. Here we demonstrate that *YKL40* expression in human livers is regulated by co-operative action of several promoter-bound transcription factors. By computational analysis and subsequent *in vitro* studies we have defined putative binding sites for NFKB subunit P65 and CEBP α in the *YKL40* promoter (Figure 3A). The NFKB pathway plays an important role in liver fibrosis, as its activation in hepatocytes can lead to activation of surrounding tissue macrophages and thus leading to fibrosis [26]. We demonstrated that TNF α mediated *YKL40* expression is regulated by P65, a component of the NOTCH/NFKB signaling pathway (Figures 2 and 3). Additionally our study demonstrates that NOTCH1 is essential for nuclear retention of P65 in human liver cells (Figure 5). Studies in animal models have shown that knockdown of *NOTCH1* resulted in impairment of DNA binding and transcriptional activation ability of P65 and impacted dendritic cell differentiation [12]. We have shown for the first time that the NFKB subunit P65 cooperates with CEBP α to regulate expression of *YKL40* through direct DNA binding in hepatocytes (Figures 3 and 4). Several studies have shown that CEBP α regulates activation of hepatic stellate cells which play key

roles in hepatic fibrosis [27,28]. Differential modulation of CEBP α has been shown in HCC patients [17,29]. Our analysis on the regulation of the inflammatory biomarker *YKL40* expression at the transcriptional level provides new insight into role of components of the NOTCH and NFKB signaling pathways in HCV induced hepatic fibrosis and HCC. It is of interest that HCV core protein NS3 can activate the NOTCH signaling pathway resulting in development of HCV-induced HCC [30]. Activation of NOTCH signaling also promotes TGF β 1 induced epithelial-mesenchymal transition, an initial step in the development of fibrosis, by directly interacting with the transcriptional machinery [31,32,33]. Modulation of both NOTCH1 and NFKB pathways have also been implicated in several cancers including HCC [34,35,36,37].

In addition to demonstrating the interaction of NOTCH, CEBP α and NFKB pathways in *YKL40* expression, we determined an important role for modulation of miRNA by HCV. The understanding of the complex role of miRNAs in the various physiological and pathological processes is still emerging. miRNAs have been implicated in regulation of pro-inflammatory cytokines, anti-inflammatory cytokines, and interferons [38]. miRNA-21 has been shown to regulate chronic rejection and has been implicated in the development of fibrosis following liver transplantation [39,40]. miRNA-21 modulates resident fibroblasts, epithelial cells and lymphocytes to produce pro-fibrotic cytokines resulting in deposition of ECM components [39,41]. It has been shown that several liver specific miRNAs including miRNA-122, miRNA-148, miRNA-194 are sensitive biomarkers for hepatocyte injury and rejection after liver transplantation [42]. In this study we identified a novel miRNA (miRNA-449a) that is modulated in HCV infection. Further, we have shown that miRNA-449a regulates HCV induced inflammatory responses (YKL40) implicated in allograft liver fibrosis.

Previous studies in our laboratory have demonstrated an upregulation of autoimmune Th17 inflammatory cascade leading to liver fibrosis in HCV infection, particularly in recurrent HCV following orthotopic liver transplantation [43]. Viral modulations of miRNA have been well known to influence transcriptional regulation in T cell responses, inflammation and fibrosis [44]. Although suggested in literature, a direct effect of HCV mediated modulation of cellular inflammatory responses and fibrosis is yet to be determined. In our current study using promoter analyses techniques we provide direct evidence for the role of miRNA-449a, which is down regulated in HCV infection (Figure 1), in the upregulation pro-inflammatory YKL40 fibrotic cascade. miRNA-449a has been implicated transcriptional dysregulation affecting cell proliferation in several human diseases including cancers [45,46]. *In vitro* studies have also shown that miRNA-449a can arrest cell proliferation and induce apoptosis [46,47]. Thus, HCV induced down regulation of miRNA-449a in human livers can upregulate transcriptional factors leading to increased inflammatory response; promoting cell proliferation that can result in HCC.

We have also demonstrated by *in vitro* analysis that miRNA-449a regulates TNF α mediated induction of *YKL40* by targeting components of the NOTCH signaling pathway (*NOTCH1*) (Figure 6). We have shown for the first time in human hepatocytes that miRNA-449a targets *NOTCH1* for translational silencing. Studies have shown that miRNA-34a is downregulated in patients with chronic hypoxia kidney diseases and promotes epithelial-mesenchymal transition by targeting components of the NOTCH signaling pathway [48]. In HCV infected patients expression of miRNA-449a was significantly downregulated (Figure 1A). In consistence with our *in vitro* results, in the same HCV patients downregulation of miRNA-449a was accompanied by significant upregulation of *NOTCH1* (Figure 7). Thus, results obtained from

patient samples and our *in vitro* analysis using hepatocytes indicate that upregulation of *NOTCH1* resulting from downregulation of miRNA-449a stabilizes nuclear P65 to activate *YKL40* expression in patients with HCV mediated hepatic fibrosis (Figure 1). The increased expression of *YKL40* in patients with HCV mediated liver fibrosis [5,6] can be attributed to this novel pathway (Figure 8). Since, *YKL40* is elevated in patients with multiple liver diseases (Figure 1B); it is likely that other parallel pathways for its transcriptional regulation may exist in non-HCV mediated liver fibrosis.

Taken together our results provide new insight into the mechanisms by which miRNAs mediate changes in the inflammatory process by modulating components of the transcriptional machinery. The results from this study should assist in the development of novel strategies for identifying non-invasive biomarkers that can prognosticate patients and monitor those at increased risk for development of cirrhosis and HCC following HCV infection.

Supporting Information

Figure S1 CEBP α interacts with P65. Co-immunoprecipitation of CEBP α with P65 in hepatocytes. Whole cell lysates were subjected to immunoprecipitation with either mouse IgG or anti-CEBP α . P65 in the cell lysates (Input) and immunoprecipitated complexes (IP) was detected by immunoblotting with anti-P65. CEBP α was detected by immunoblotting with anti-CEBP α . (TIF)

References

- Alter MJ, Kruszon-Moran D, Nainan OV, McQuillan GM, Gao F, et al. (1999) The prevalence of hepatitis C virus infection in the United States, 1988 through 1994. *N Engl J Med* 341: 556–562.
- Lauer GM, Walker BD (2001) Hepatitis C virus infection. *N Engl J Med* 345: 41–52.
- Seeff LB (2002) Natural history of chronic hepatitis C. *Hepatology* 36: S35–46.
- Volck B, Price PA, Johansen JS, Sorensen O, Benfield TL, et al. (1998) YKL-40, a mammalian member of the chitinase family, is a matrix protein of specific granules in human neutrophils. *Proc Assoc Am Physicians* 110: 351–360.
- Johansen JS, Christoffersen P, Moller S, Price PA, Henriksen JH, et al. (2000) Serum YKL-40 is increased in patients with hepatic fibrosis. *J Hepatol* 32: 911–920.
- Lee CG, Da Silva CA, Dela Cruz CS, Ahangari F, Ma B, et al. (2011) Role of chitin and chitinase/chitinase-like proteins in inflammation, tissue remodeling, and injury. *Annu Rev Physiol* 73: 479–501.
- Stevens AL, Wishnok JS, Chai DH, Grodzinsky AJ, Tannenbaum SR (2008) A sodium dodecyl sulfate-polyacrylamide gel electrophoresis-liquid chromatography tandem mass spectrometry analysis of bovine cartilage tissue response to mechanical compression injury and the inflammatory cytokines tumor necrosis factor alpha and interleukin-1beta. *Arthritis Rheum* 58: 489–500.
- Ladner KJ, Caligiuri MA, Guttridge DC (2003) Tumor necrosis factor-regulated biphasic activation of NF-kappa B is required for cytokine-induced loss of skeletal muscle gene products. *J Biol Chem* 278: 2294–2303.
- Caamano J, Hunter CA (2002) NF-kappaB family of transcription factors: central regulators of innate and adaptive immune functions. *Clin Microbiol Rev* 15: 414–429.
- Fullard N, Wilson CL, Oakley F (2012) Roles of c-Rel signalling in inflammation and disease. *Int J Biochem Cell Biol*.
- Cao Q, Li P, Lu J, Dheen ST, Kaur C, et al. (2010) Nuclear factor-kappaB/p65 responds to changes in the Notch signaling pathway in murine BV-2 cells and in amoeboid microglia in postnatal rats treated with the gamma-secretase complex blocker DAPT. *J Neurosci Res* 88: 2701–2714.
- Cheng P, Zlobin A, Volgina V, Gottipati S, Osborne B, et al. (2001) Notch-1 regulates NF-kappaB activity in hemopoietic progenitor cells. *J Immunol* 167: 4458–4467.
- Shin HM, Minter LM, Cho OH, Gottipati S, Fauq AH, et al. (2006) Notch1 augments NF-kappaB activity by facilitating its nuclear retention. *EMBO J* 25: 129–138.
- Hacker H, Karin M (2006) Regulation and function of IKK and IKK-related kinases. *Sci STKE* 2006: re13.
- Johnson PF (2005) Molecular stop signs: regulation of cell-cycle arrest by C/EBP transcription factors. *J Cell Sci* 118: 2545–2555.

Figure S2 siRNA mediated knockdown of NOTCH1. A. Hepatocytes were transfected with either non-specific siRNA or siRNA specific for NOTCH1 and treated with TNF α . Lysates were subjected to immunoblotting with anti-NOTCH1. B. HEPG2 cells were transfected with either non-specific siRNA or siRNA specific for NOTCH1, treated with TNF α and immunostained with anti-NOTCH1. C. Quantification of the NOTCH1 immunostaining signal in HEPG2 cells (S2B). The numbers represent the average fluorescence intensity of P65 (n = 100). (TIF)

Figure S3 miRNA-449a regulates YKL40 expression. Hepatocytes were transfected with an empty vector (-) or vector expressing miRNA-449a (+) and expression of *YKL40* was determined by Q-PCR. The $\Delta\Delta CT$ value was calculated by normalizing the threshold (CT) values with *GAPDH* and expression of *YKL40* in controls. The * represents p value < 0.05 obtained by a two-tailed t-test. (TIF)

Acknowledgments

The authors thank Ms. Billie Glasscock for her help in preparing this manuscript.

Author Contributions

Conceived and designed the experiments: NS TM. Performed the experiments: NS VT. Analyzed the data: NS. Contributed reagents/materials/analysis tools: NS VS SS JC WC. Wrote the paper: NS TM.

- Zeng C, Wang R, Li D, Lin XJ, Wei QK, et al. (2010) A novel GSK-3 beta-C/EBP alpha-miR-122-insulin-like growth factor 1 receptor regulatory circuitry in human hepatocellular carcinoma. *Hepatology* 52: 1702–1712.
- Lu GD, Leung CH, Yan B, Tan CM, Low SY, et al. (2010) C/EBPalpha is up-regulated in a subset of hepatocellular carcinomas and plays a role in cell growth and proliferation. *Gastroenterology* 139: 632–643, 643 e631–634.
- McManus MT (2003) MicroRNAs and cancer. *Semin Cancer Biol* 13: 253–258.
- Gracias DT, Katsikis PD (2011) MicroRNAs: key components of immune regulation. *Adv Exp Med Biol* 780: 15–26.
- Miska EA (2005) How microRNAs control cell division, differentiation and death. *Curr Opin Genet Dev* 15: 563–568.
- Girard M, Jacquemin E, Munnich A, Lyonnet S, Henrion-Caude A (2008) miR-122, a paradigm for the role of microRNAs in the liver. *J Hepatol* 48: 648–656.
- Sarma NJ, Yaseen NR (2011) Amino-terminal enhancer of split (AES) interacts with the oncoprotein NUP98-HOX9A and enhances its transforming ability. *J Biol Chem* 286: 38989–39001.
- Kamal SM, Turner B, He Q, Rasenack J, Bianchi L, et al. (2006) Progression of fibrosis in hepatitis C with and without schistosomiasis: correlation with serum markers of fibrosis. *Hepatology* 43: 771–779.
- Pungpapong S, Nunes DP, Krishna M, Nakhleh R, Chambers K, et al. (2008) Serum fibrosis markers can predict rapid fibrosis progression after liver transplantation for hepatitis C. *Liver Transpl* 14: 1294–1302.
- Xiao XQ, Hassanein T, Li QF, Liu W, Zheng YH, et al. (2011) YKL-40 expression in human hepatocellular carcinoma: a potential biomarker? *Hepatobiliary Pancreat Dis Int* 10: 605–610.
- Sunami Y, Leithauser F, Gul S, Fiedler K, Guldiken N, et al. (2012) Hepatic activation of IKK/NF-kappaB signaling induces liver fibrosis via macrophage-mediated chronic inflammation. *Hepatology*.
- Huang J, Zhang JS, Huang GC, Tang QQ, Chen C, et al. (2004) [Expression of CCAAT/enhancer-binding protein in cultured rat hepatic stellate cells and its significance]. *Zhonghua Gan Zang Bing Za Zhi* 12: 259–262.
- Tao LL, Cheng YY, Ding D, Mei S, Xu JW, et al. (2012) C/EBP-alpha ameliorates CCl(4)-induced liver fibrosis in mice through promoting apoptosis of hepatic stellate cells with little apoptotic effect on hepatocytes *in vitro* and *in vivo*. *Apoptosis*.
- Tseng HH, Hwang YH, Yeh KT, Chang JG, Chen YL, et al. (2009) Reduced expression of C/EBP alpha protein in hepatocellular carcinoma is associated with advanced tumor stage and shortened patient survival. *J Cancer Res Clin Oncol* 135: 241–247.
- Iwai A, Takegami T, Shiozaki T, Miyazaki T (2011) Hepatitis C virus NS3 protein can activate the Notch-signaling pathway through binding to a transcription factor, SRCAP. *PLoS One* 6: e20718.

31. Saad S, Stanners SR, Yong R, Tang O, Pollock CA (2010) Notch mediated epithelial to mesenchymal transformation is associated with increased expression of the Snail transcription factor. *Int J Biochem Cell Biol* 42: 1115–1122.
32. Matsuno Y, Coelho AL, Jarai G, Westwick J, Hogaboam CM (2012) Notch signaling mediates TGF-beta1-induced epithelial-mesenchymal transition through the induction of Snail. *Int J Biochem Cell Biol* 44: 776–789.
33. Bielez B, Sirin Y, Si H, Niranjan T, Gruenwald A, et al. (2010) Epithelial Notch signaling regulates interstitial fibrosis development in the kidneys of mice and humans. *J Clin Invest* 120: 4040–4054.
34. Lim SO, Park YM, Kim HS, Quan X, Yoo JE, et al. (2011) Notch1 differentially regulates oncogenesis by wildtype p53 overexpression and p53 mutation in grade III hepatocellular carcinoma. *Hepatology* 53: 1352–1362.
35. Wumbach E, Chen YB, Khitrov G, Zhang W, Roayaie S, et al. (2007) Genome-wide molecular profiles of HCV-induced dysplasia and hepatocellular carcinoma. *Hepatology* 45: 938–947.
36. Lobry C, Oh P, Aifantis I (2011) Oncogenic and tumor suppressor functions of Notch in cancer: it's NOTCH what you think. *J Exp Med* 208: 1931–1935.
37. Liu Y, Lou G, Wu W, Zheng M, Shi Y, et al. (2011) Involvement of the NF-kappaB pathway in multidrug resistance induced by HBx in a hepatoma cell line. *J Viral Hepat* 18: e439–446.
38. McCoy CE (2012) The role of miRNAs in cytokine signaling. *Front Biosci* 17: 2161–2171.
39. Marquez RT, Bandyopadhyay S, Wendlandt EB, Keck K, Hoffer BA, et al. (2010) Correlation between microRNA expression levels and clinical parameters associated with chronic hepatitis C viral infection in humans. *Lab Invest* 90: 1727–1736.
40. Bihrer V, Waidmann O, Friedrich-Rust M, Forestier N, Susser S, et al. (2011) Serum microRNA-21 as marker for necroinflammation in hepatitis C patients with and without hepatocellular carcinoma. *PLoS One* 6: e26971.
41. Liu G, Friggeri A, Yang Y, Milosevic J, Ding Q, et al. (2010) miR-21 mediates fibrogenic activation of pulmonary fibroblasts and lung fibrosis. *J Exp Med* 207: 1589–1597.
42. Farid WR, Pan Q, van der Meer AJ, de Ruiter PE, Ramakrishnaiah V, et al. (2011) Hepatocyte-derived micromas as serum biomarker of hepatic injury and rejection after liver transplantation. *Liver Transpl*.
43. Basha HI, Subramanian V, Seetharam A, Nath DS, Ramachandran S, et al. (2011) Characterization of HCV-specific CD4+Th17 immunity in recurrent hepatitis C-induced liver allograft fibrosis. *Am J Transplant* 11: 775–785.
44. Cermelli S, Ruggieri A, Marrero JA, Ioannou GN, Beretta L (2011) Circulating microRNAs in patients with chronic hepatitis C and non-alcoholic fatty liver disease. *PLoS One* 6: e23937.
45. Noonan EJ, Place RF, Pookot D, Basak S, Whitson JM, et al. (2009) miR-449a targets HDAC-1 and induces growth arrest in prostate cancer. *Oncogene* 28: 1714–1724.
46. Noonan EJ, Place RF, Basak S, Pookot D, Li LC (2010) miR-449a causes Rb-dependent cell cycle arrest and senescence in prostate cancer cells. *Oncotarget* 1: 349–358.
47. Lize M, Pilarski S, Dobbstein M (2010) E2F1-inducible microRNA 449a/b suppresses cell proliferation and promotes apoptosis. *Cell Death Differ* 17: 452–458.
48. Du R, Sun W, Xia L, Zhao A, Yu Y, et al. (2012) Hypoxia-induced down-regulation of microRNA-34a promotes EMT by targeting the Notch signaling pathway in tubular epithelial cells. *PLoS One* 7: e30771.